Propellants,
Explosives,
Pyrotechnics

Full Paper

Afterburn Ignition Delay and Shock Augmentation in Fuel Rich Solid Explosives

Kevin L. McNesby,* Barrie E. Homan, John J. Ritter, Zachary Quine, Rachel Z. Ehlers, Brendan A. McAndrew

U.S. Army Research Laboratory, Aberdeen Proving Ground, MD 21005-5066 (USA)

Received: September 18, 2008; revised version: July 23, 2009

DOI: 10.1002/prep.200800084

Abstract

We present experimental and computational results that explain some aspects of measured energy release in explosions of unconfined trinitrotoluene [TNT, $C_6H_2(NO_2)_3CH_3$], and an aluminum-containing explosive formulation, and show how this energy release can influence shock wave velocities in air. In our interpretation, energy release is divided into early, middle, and late time regimes. An explanation is provided for the interdependence of the time regimes and their influence on the rate at which energy (detonation/explosion and afterburn) is released. We use a merging of the thermodynamic and chemical kinetic processes that predicts how chemical kinetics may determine the time delay of the afterburn of combustible gases produced by the initial detonation/explosion/fast reaction. The thermodynamic computer code CHEETAH is used to predict gaseous and solid products of early time energy release, and a chemical kinetic reaction mechanism (CHEMKIN format) is used to describe the subsequent afterburn of the gas phase products in air. Results of these calculations are compared with field measurements of unconfined explosions of 2 kg charge weights of TNT and an aluminum-containing explosive formulation.

Keywords: Chemical Kinetics, Energy Management, Explosives, Ignition Delay, Shock Augmentation

1 Introduction

The hazards encountered by an object in the vicinity of an explosion produced by the fuel-rich secondary high explosive material trinitrotoluene [TNT, $C_6H_2(NO_2)_3CH_3$] have been extensively studied and well documented [1 – 3]. For a TNT explosion, energy is released in stages. The first energy release, referred to as detonation energy, is produced by fast chemical reactions involving intramolecular bond breaking ($C{-}NO_2$, $C{-}CH_3$) in the solid explosive. This is immediately followed by a slightly longer duration, lower intensity energy release from dense-gas bimolecular reactions occurring initially between fuel ($-CH_x$) and oxidizer ($-NO_2$) components liberated within the TNT molecule by the detonation [4]. This combined energy release is dominated by the detonation energy, is complete within microseconds of initiation, and is not dependent upon any outside chemical ingredients. In what follows, we categorize this time region as the early time following initiation. Further energy is also available on a much longer timescale, corresponding to the burning of the fuel-rich early time products in air, and in what follows, we categorize this as middle and late time energy release. These latter processes, lasting to many milliseconds after initiation, are usually referred to in the literature [3] as afterburning.

As an example of the potential importance of afterburning to total energy release, the energy of detonation of TNT is $\sim$4600 J g^{-1}. Detonation products are mainly solid carbon, CO, CO_2, N_2, and H_2O. These detonation products, when mixed with air and fully combusted, yield $\sim$10040 J g^{-1}, or more than twice the energy of detonation [1]. This additional energy is often not realized for explosions of unconfined TNT due to several factors, including isentropic expansion, mixing efficiency with air, and the ignition temperature of the fuel and air mixture. It is important to note that the combustion energy from TNT detonation products is available on the millisecond combustion time scale rather than the microsecond time scale of detonation. This paper describes our efforts to use mainly optical methods to categorize time regions of energy release and provide additional insight into the afterburning process in TNT. This paper describes an investigation of the potential importance of chemical kinetics to afterburn energy, the influence on shock velocity, and proposes a more detailed definition of an enhanced blast. Finally, we propose a possible route for achieving an enhanced blast in an unconfined explosive formulation.

2 Background

There are many detailed studies of detonation in solid explosives and in TNT in particular [2]. Studies of afterburning in TNT, and in most condensed explosives, have

* Corresponding author; e-mail address: mcnesby@arl.army.mil.

been much less extensive. Modern investigations into afterburning with applicability to TNT explosions approximately begin with measurements by Gaydon of CO and C_2 spectra in hydrocarbon/air explosions [5]. For "violent" hydrocarbon/air explosions in closed vessels, the appearance of the CO flame spectrum was attributed to the afterburning of fuel gases. More recently, Kuhl has developed a theoretical model, with complementary experimental work, of afterburning in explosions created by turbulent mixing of the detonation products from fuel-rich charges with air [6]. This model uses a thermodynamic-equilibrium description combined with a gas dynamic treatment of the flow field within a closed vessel, and provides a time-resolved prediction of detonation product gas mixing with air, combustion, and equilibration. Gel'fand has used a pyrometric technique for examining afterburning in the absence of turbulent mixing or reflected shock for 100 g samples of TNT and TNT/nitramine mixtures. Temperature measurements indicate the importance of unburned fuel (C and CO) in late time energy release. The importance of turbulent mixing and the possibility of tailoring the detonation product gases for achieving maximum afterburn is mentioned [7].

3 Approach

The goal of the work described here is to begin to understand how products and temperatures of early time chemical reaction and energy release in some solid explosives affect middle and late time chemical reaction and energy release, and to use this knowledge to predict any shock velocity augmentation, and promptness of energy of afterburn. The approach uses detailed measurements of shock velocity and temperature of explosions to define time regions of energy release and simple thermodynamic and kinetic calculations to demonstrate the potential importance of chemical kinetics to afterburning. The chemical kinetic calculations are simplistic in that they are not combined with fluid dynamics to predict mixing in the complex environment of the expanding detonation products. Nevertheless, we believe this work shows how early time chemical species and temperatures may influence total energy release, potentially enabling dynamic energy control in some explosive formulations.

4 Experimental Facilities

The full instrumentation suite used to characterize open air explosions has been described in detail in previous DoD publications [8–10], but is described briefly here for those unable to access these documents. Figure 1 shows an overhead diagram of the experimental facility at the Aberdeen Proving Ground (APG), and an insert photograph of the reflective material attached to the rearmost barrier wall as viewed from the instrument enclosure. For the results presented here, we rely on data measured using high brightness imaging and multicolor pyrometry. Methods of data collection and analysis have also been described in detail previously [11–13]. Briefly, high brightness imaging uses a high power, high repetition rate Cu-vapor laser (1 mJ pulse^{-1}, $\geq$20 kHz, 10 ns pulse^{-1}, Oxford Lasers, Inc.), synchronized to a filtered, high speed digital camera (Vision Research, Inc.). The laser is used to illuminate a barrier wall covered with reflective material. The explosive is placed between the laser source and the reflective wall. Regions of the explosive and fireball are shadow-imaged at the laser

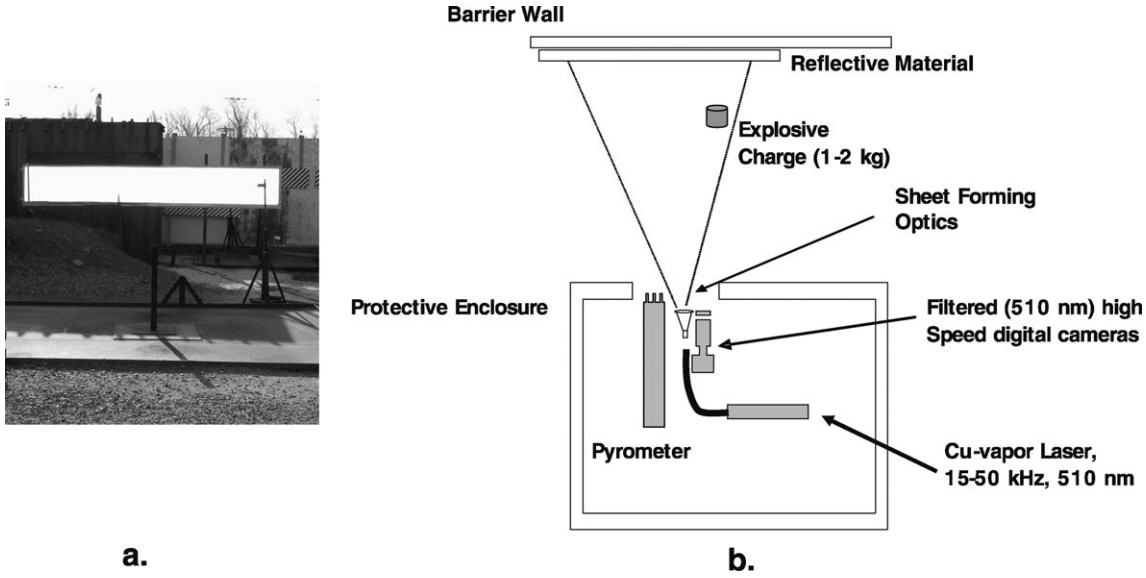

Figure 1. (a) A photograph of the reflective material taken from the location of the Cu-vapor laser source and optical pyrometer, located within the protective enclosure. (b) A schematic (not to exact scale), looking from above, of the equipment layout at the outdoor experimental facility.

wavelength, and the laser pulse is synchronized to the camera shutter. This technique discriminates against the optical emission from the explosive, allowing structures at the edge of the fireball to be imaged. This technique allows images of early time (< 200 μs) fractionation of the explosive material, imaging of particulates exterior to the fireball, and imaging of turbulent mixing and shock front near the surface of the fireball. From these images it is possible to measure the velocity of the leading shock and the velocity of the expansion of the fireball, and measure separation between the leading shock and the contact surface of the fireball [11]. Typical imaging rates are from 12000 to 50000 images s^{-1}, with an exposure time per image of $2 - 10$ μs. The apparent "thickness" of the shock region seen in these images is likely caused by light refraction by the curved contour of the shock front.

The pyrometer system, developed and built at the Army Research Laboratory (ARL), is a 3-color system. The pyrometer consists of a series of diode-terminated (Newport Corp.) 600 μm-core Si–Si optical fibers (Aurora Optics) coupled with 10 nm bandpass filters in the visible to near infrared region (700, 820, and 900 nm, Newport Corp.). The three fibers have an acceptance angle of $\sim 22^{\circ}$, and are placed within the main instrument enclosure ~ 15 m from the center of the explosive charge. The central line of sight of each fiber is aimed at the center of the explosive charge. At this distance from the charge, the fiber "sees" light emitted from the entire fireball, so the temperatures reported are integrated over the full fireball surface at all times. The current system has a 13 μs risetime. Calibration prior to measurement was performed against a standard blackbody (Newport Corp.), a calibrated visible emission lamp (Ocean Optics, Inc.), and against solar emission. For the measurements reported here, the temperature is that of the visible surface of the fireball. Emissivity is assumed to be constant (graybody assumption). Temperature uncertainty is estimated to be ± 100 K [11].

For calculations used to predict afterburn species and temperatures, we employ the CHEETAH explosive performance predictive computer program (Lawrence Livermore National Laboratory) to estimate early time to middle time detonation product temperatures and species, and use the CHEMKIN combustion computer code (Reaction Design, Inc.) to predict late time ignition delays and products of gaseous detonation product/air combustion. The chemical species input to CHEMKIN are those predicted by CHEETAH. The chemical combustion mechanism used in the CHEMKIN code includes Gas Research Institute GRIMECH 3.0, Sandia National Laboratory and Lawrence Livermore National Laboratory mechanisms for hydrocarbon combustion, and mechanisms compiled for combustion of nitrated hydrocarbons [14]. The chemical mechanism consists of 249 species and 2032 reactions. All reactants and reactions input to the CHEMKIN code are in the gas phase. It should be emphasized that all computational results presented here are based upon a closed, gas phase homogeneous reactor model, and that fluid dynamic effects are not considered, nor is heterogeneous combustion (i.e., combustion of solid carbon particles). Efforts are currently underway to incorporate chemical kinetics and heterogeneous combustion into fluid dynamic models of the systems described here.

5 Results and Discussion

5.1 Time Regimes

Figure 2 shows a sequence of high brightness images during explosion of an unconfined 2 kg TNT charge. The charge was supported 2 m above the ground on a styrofoam stand, the horizontal field of view is ~ 3 m, and the exposure time of each image is 2 μs. The first frame at the top of Figure 2 is unlabeled and shows the charge prior to initiation, with the laser-illuminated screen in the background. The second frame, labeled 0 s with the legend "Early Time" shows the top-detonated charge as the detonation travels downward through the solid explosive. As the detonation finishes in the solid material and the shock wave transitions to air, the dense detonation products of TNT expand isentropically, the bulk detonation products react anaerobically, and detonation products at the surface of the dense expanding cloud react with air. CHEETAH calculations indicate that the chemical composition of the detonation products is fixed when the detonation product cloud reaches approximately two initial charge diameters. The fixing, or "freeze out" of the chemical composition of the detonation products is used in this analysis as the end of the early time energy release.

The third frame in Figure 2, labeled 0.000125 s with the legend "Middle Time" shows hot detonation products expanding into the surroundings following completion of detonation and freeze out. In this analysis, the onset of the middle time coincides with the beginning of afterburning. The leading shock is at the surface of the cloud of expanding detonation products. In the image labeled Middle Time in

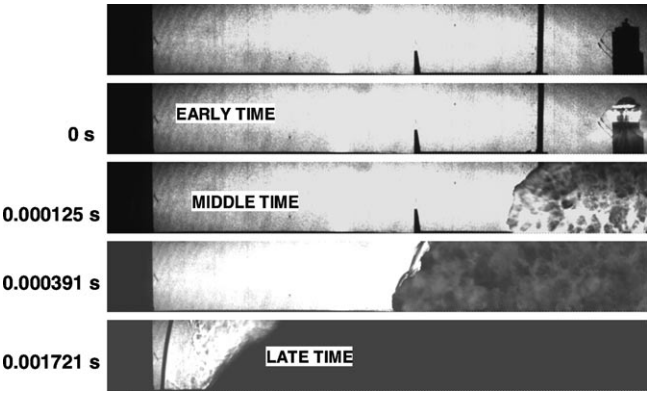

Figure 2. A sequence of high brightness images of a functioning 2 kg mass of TNT (unconfined). The light reaching the camera is at 510 nm (2 nm bandwidth), and is reflected back to the camera by the reflective material attached to the barrier wall. Some of the emission visible in the frame labeled "early time" may be from shock compressed air.

Figure 2, the detonation products have expanded to ~5 charge diameters. Thermal emission from hot carbon particles and hot detonation product gases is intense, as can be seen by the emission intensity in this figure being near that of the scattered laser light at 510 nm. The interior of the expanding cloud is cooling and mixing with air begins to occur in the cloud interior on a bulk scale. The detailed chemical makeup and temperature of the detonation products become important in determining the extent of afterburning. It is important to emphasize that the energy release during this time region may be highly complex and governed by turbulent mixing, with significant temperature and pressure gradients within the detonation product cloud – air mixture. In the middle time, aerobic burning at the interface of the expanding detonation product cloud, and within the bulk gas mixture, may significantly contribute to thermal emission and augment the shock velocity. For distances from the original explosive center up to many (~10) charge diameters, the velocity of the detonation products is similar to the leading shock, i.e., the launched (leading) shock is riding on the surface of this expanding detonation product cloud. As the explosive products continue to expand and cool, drag forces and decreasing temperatures cause the expansion rate of the detonation product – air mixture cloud to decrease faster than does the leading shock velocity, and the emission of light near 510 nm decreases. In Figure 2, at the image labeled 0.000391 s, the leading shock separates from the surface of the detonation product cloud and continues traveling outward from the original location of the explosion. This time of separation defines the end of the middle time chemical reaction and energy release in this analysis.

As the detonation product cloud cools, it asymptotically approaches a final diameter, thermal emission decreases, and bulk mixing with the surrounding environment becomes most important to energy release. The fifth frame in Figure 2, labeled 0.001721 s with the legend "Late Time", shows the leading shock well separated from the detonation product cloud. The leading shock separation and onset of bulk mixing with air signifies the beginning of the late time stage of energy release, and is usually referred to as the afterburn, although we maintain the afterburn begins with the onset of the middle time. In our analysis, afterburning begins tens of microseconds after initiation and continues to tens of milliseconds. For TNT, and most condensed explosives, open air explosions exhibit limited afterburning, relative to explosions in confined areas. Explosions occurring in confined spaces may show enhanced afterburning, mainly as a result of the leading shock being reflected back into the detonation product/air mixture, causing heating and promoting mixing.

5.2 Measured Temperatures and Fireball Radius

Figure 3 shows the measured emission intensity at 820 nm (10 nm bandwidth) reported by a single channel of the pyrometer from a 2 kg TNT charge functioning as in Figure 2. This figure is similar to that found in Ref. [7] and shows a time separation between an intense, short duration light output near the time of initiation and a long duration light pulse that begins a few milliseconds after initiation and peaks ~20 ms after initiation. The intense, short duration light output is a convolution of the early time energy release (detonation and freeze out) and subsequent cooling and middle time energy release corresponding to the onset of afterburn. The longer duration pulse is light emitted during the late-time afterburn as the fireball approaches its final diameter. These emission data agree reasonably well with the images in Figure 2.

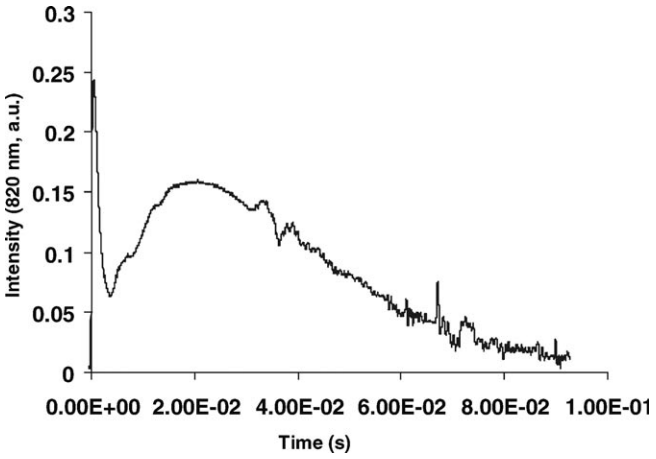

Figure 3. The measured emission intensity at 820 nm reported by a single channel of the pyrometer from a 2 kg TNT charge (unconfined). Note the spike of light intensity corresponding to early and middle time energy release and the long duration of late time energy release. The single channel output is not corrected for fireball diameter.

Figure 4 shows the measured fireball surface temperature and radius as a function of time for a TNT explosion, and the fireball surface temperature for the aluminized high explosive PBXN-109. Fireball surface temperatures were mea-

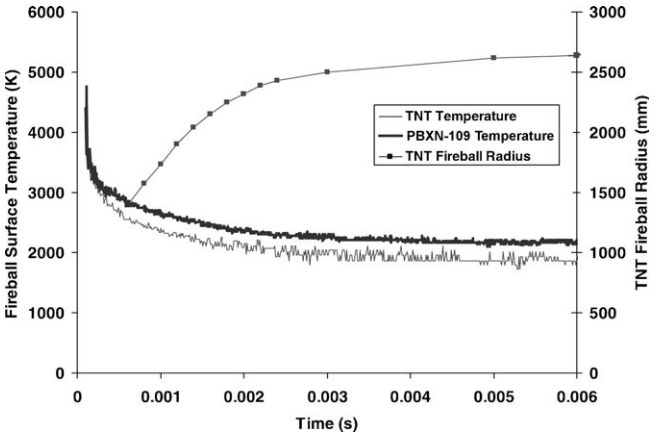

Figure 4. Measured fireball radius and measured surface temperature for TNT, and measured surface temperature for PBXN-109, with suggested time regions. Approximately 2 kg charge weight, unconfined.

sured with the 3-color pyrometer, the fireball radius was measured from visual records similar to those shown in Figure 2. Figure 4 is in some disagreement with that shown in Ref. [7] in that our measured temperature for TNT (and for PBXN-109) remains relatively constant (actually slightly decreasing) in the beginning of the late time region (times greater than 1 ms), even though single channel light intensity in Figure 3 begins to increase. We have interpreted this result based on a flamelet model of afterburning [15], in which the afterburning at the surface consists of flamelets of fuel and oxidizer, each burning at similar temperatures. In this case the number of flamelets will determine the intensity, but the overall temperature is relatively constant.

5.3 Calculated Afterburn Ignition Delay for a Homogeneous System

The approach to begin to understand onset of afterburn may be summarized as follows. CHEETAH is used to calculate early time products of detonation and then to freeze their composition at a predetermined temperature limit. These products are then allowed to mix homogeneously with air and CHEMKIN is used to simulate combustion corresponding to middle and late time energy release. The temperature at which detonation product gases cease to react with each other (freeze out) may be set within the CHEETAH calculation. Typically, CHEETAH assumes product composition to be fixed once the detonation product gases reach 1800 K. Figure 5 shows the calculated final composition of gaseous detonation products of TNT for freeze out temperatures from 1200 to 2200 K. The average of the main product gas, CO, is closest to the amount predicted at 1800 K, so for the calculations that follow we use this as the freeze out temperature. The pyrometry results of Figure 4, correlated with imaging results of Figure 2, show a surface temperature near 2400 K when the shock separates from the fireball, but this is the combustion temperature at the interface of the detonation products and air, and is probably higher than the interior temperature of the detonation product cloud.

The detonation product composition at 1800 K is used as the fuel component in the CHEMKIN calculations that simulate fuel/air combustion. The calculations use a homogeneous reactor model, equal volumes of fuel and air, and a range of initial temperatures. This approach to begin to understand chemical reaction and energy release in the afterburn is oversimplified because we neglect turbulent mixing and temperature gradients that undoubtedly occur as the fireball expands into and mixes with air. We use this approach because exploring this well-mixed regime demonstrates the importance of thermochemistry and chemical kinetics to the energy release by decoupling mixing effects.

As mentioned above, a range of initial temperatures of the homogeneous fuel/air mixture is used in CHEMKIN to calculate the ignition delay of the mixture. Ignition delay is important because the faster the early to middle time detonation products begin to burn, the more likely they are to be able to support the leading shock. The ignition delay is estimated to be the time to peak OH concentration, because this value may be easily determined. Calculated temperature histories may also be used, and Figure 6 shows how the calculated OH and temperature profiles overlap. This figure shows the result of a calculation of time versus temperature and OH concentration for a well mixed TNT detonation product gas/air mixture with an initial bulk temperature of 1060 K. This initial temperature was chosen for this figure because it yields a combustion temperature close to 2450 K, near that of the experimentally measured middle time temperatures in Figure 4. Table 1 shows the temperature–time history for mixtures of TNT detonation product gases/air at several different initial temperatures. The ignition delay is based on the initial temperature in the region near the onset of combustion, while the final flame temperature is a near linear function of the explosive product/air mixture initial temperature once combustion begins. At present we do not have an explanation for the

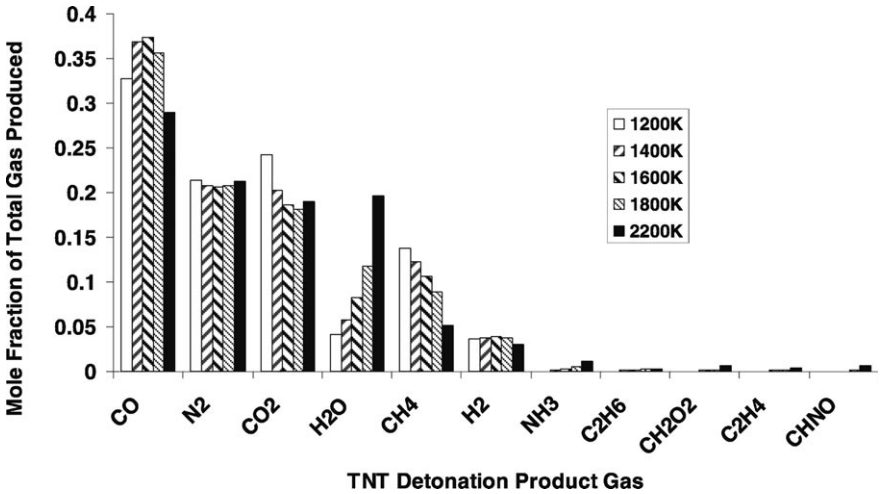

Figure 5. Detonation product gases for TNT with freeze out temperatures adjusted from 1200 to 2200 K, as predicted by CHEETAH.

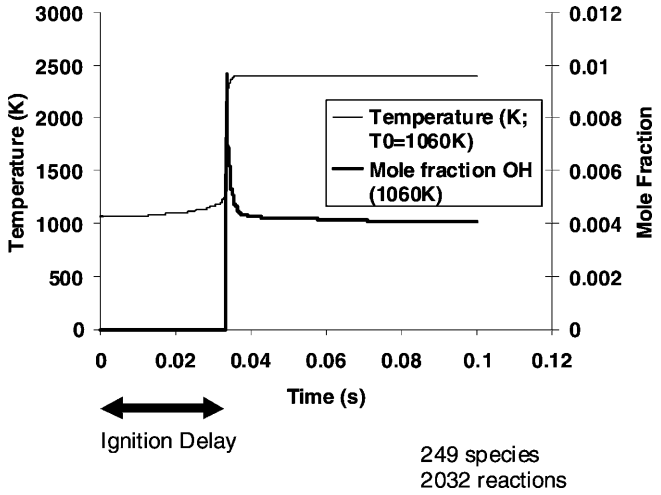

Figure 6. Calculated OH concentration and temperature versus time for an equal volume mixture of TNT detonation product gases and air with an initial temperature of 1060 K. The ignition delay as reported for these calculations is the time to peak OH concentration, although time to maximum slope of temperature change rate gives similar values.

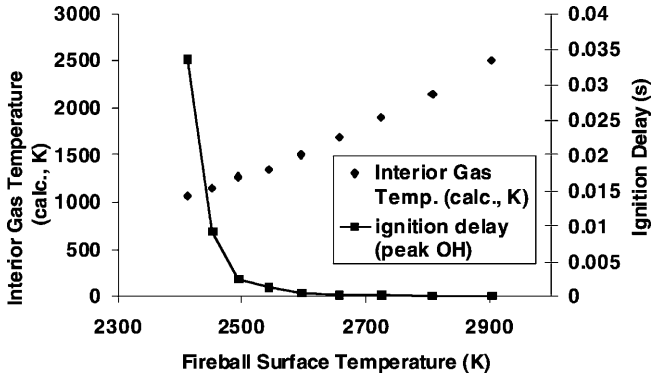

Figure 7. Calculated fireball surface temperature and calculated ignition delay for various interior gas temperatures, for equal volume TNT detonation product gas/air mixtures. As the pre-ignition temperature increases, the ignition delay decreases and the mixture burns hotter.

slight increase in calculated ignition delay at 1800 K, relative to 1600 K.

5.4 Estimation of Fireball Interior Temperatures

The CHEMKIN calculations yield an estimated combustion temperature and ignition delay based on initial temperature of a non-combusting, premixed gas. An initial estimate of temperature prior to combustion, near the surface of a well-mixed detonation product cloud/air mixture, may be inferred by comparing the temperature calculated for the combustion with experimental fireball surface temperature measurements.

Figure 7 shows the calculated fireball temperatures and the calculated ignition delays for equal volume TNT detonation product gas/air mixtures for various initial gas temperatures. In the treatment here we correlate the calculated fireball temperatures with the measured surface fireball temperatures and the initial gas temperatures with unburned gases near the surface of the fireball. This figure shows that as the unburned, interior gas temperature increases, the fireball surface temperature increases, and also shows that there is a non-linear inverse correlation between ignition delay and fireball surface temperature. So as the unburned, interior gas mixture gets hotter, it begins to burn faster, and reaches a higher combustion temperature.

Using Figure 7 as the basis for a look-up table with measured fireball surface temperature, the ignition delay of the unburned detonation product/air mixture near the fireball surface may be inferred. Figure 8 shows a plot of experimental data of shock and fireball radius and calculated ignition delay versus time after initiation for a 2 kg charge weight of TNT. It is interesting to note that the region of shock detachment from the fireball occurs in the region where the predicted ignition delay goes to larger values. A possible interpretation of this is that middle time ignition at the interface of the detonation product gas and the surrounding air must be fast in order to provide support to the leading shock.

Table 1. Variation in the calculated ignition delay and fireball surface (final) temperature for equal volume mixtures of TNT detonation product gases/air at different interior gas (initial) temperatures. These data are represented graphically in Figure 7.

Interior Gas Temperature (K)	Ignition Delay (Time to Peak OH) (s)	Fireball Surface Temperature (K)
950	No Ignition	974.9
975	No Ignition	1085.9
1000	0.01074	2417
1025	0.01016389	2434
1050	0.0047	2451
1075	0.00326	2468
1100	0.00234	2484
1150	0.00128	2516
1200	0.00076	2570
1400	0.00018	2655
1600	8.00E-05	2747
1800	0.00014	2699

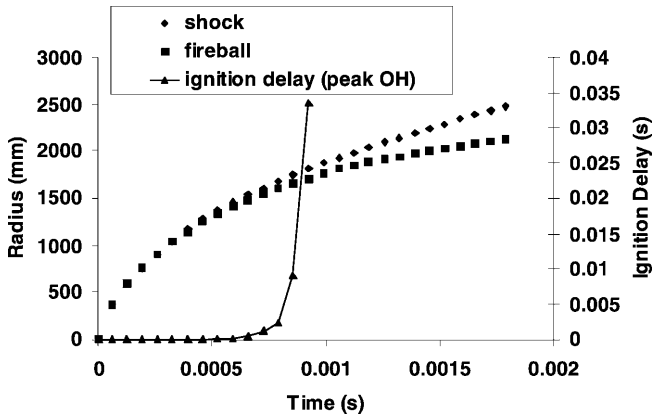

Figure 8. Measured shock and fireball radius and calculated ignition delay versus time after initiation for TNT.

5.5 Comparison to PBXN-109

PBXN-109 is a metalized explosive composed mainly of RDX and aluminum. Figure 4 shows that for similar charge masses, PBXN-109 exhibits a slightly higher fireball surface temperature than TNT. Figure 9 shows a comparison of measured shock velocities for ~2 kg charges of TNT and PBXN-109 as a function of distance from the charge center. The distance is scaled to account for the slight mass difference between the two charges. The shock velocities are derived from high brightness imaging visual records, so the velocities between 0 and 0.2 are not shown because of the inability to synchronize the initiation of the charge exactly with a laser pulse. Figure 9 shows that the leading shock velocity corresponding to "middle time" (near a scaled distance of 1.0) is enhanced for PBXN-109 relative to TNT. To express this in another way, the leading shock from PBXN-109 decelerates at a slower rate than for TNT. We believe that this enhancement of shock velocity at middle times may be a real metric for enhanced blast.

Figure 10 shows the results of a CHEETAH calculation predicting detonation product gases at a freeze out temperature of 1800 K for PBXN-109 and for TNT. For this calculation, the Al was assumed to be active (as opposed to inert). This means that the Al was allowed to compete for oxygen during the detonation. When the Al powder participates fully in early time energy release, the PBXN-109 is predicted to produce over six times the amount of hydrogen gas produced by TNT per mole of explosive. Detonation product gas/air mixtures for PBXN-109 were incorporated into the closed homogeneous reactor model in CHEMKIN. Figure 11, analogous to Figure 7, shows calculated fireball temperatures and calculated ignition delays for equal volume PBXN-109 detonation product gas/air mixtures for various initial gas temperatures. Using the approach described for TNT, Figure 11 is used as the basis for a look-up table, with measured PBXN-109 fireball surface temperatures, to estimate the ignition delay of the unburned PBXN-109 detonation product/air mixture near the fireball surface. Figure 12, analogous to Figure 8, shows a plot of experimental data of shock and fireball radius and calculated ignition delay versus time after initiation for a 2 kg charge weight of PBXN-109. The ignition delay for this mixture remains small (relative to TNT) in the region where shock velocity enhancement was shown (see Figure 8). As the PBXN-109 fireball reaches a finite size, the leading shock must detach, but this occurs later in the middle time than for TNT. Figure 13 shows a graph of calculated ignition delay for homogeneous detonation product gas/air mixtures for TNT and for PBXN-109 over a range of temperatures. In general, to achieve a given ignition delay, the detonation product gas/air mixture must be hotter for TNT than for

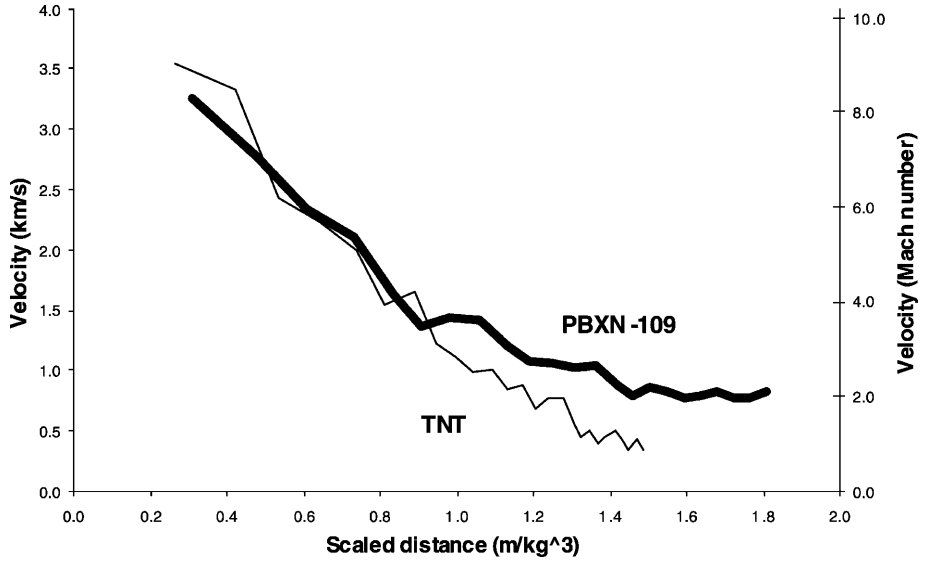

Figure 9. Measured shock velocities for ~2 kg charges of PBXN-109 and TNT. Note the middle time (scaled distance near 1.0) shock velocity enhancement for PBXN-109, relative to TNT. Scaled distances were used to account for minor differences (< 10%) between charge weights.

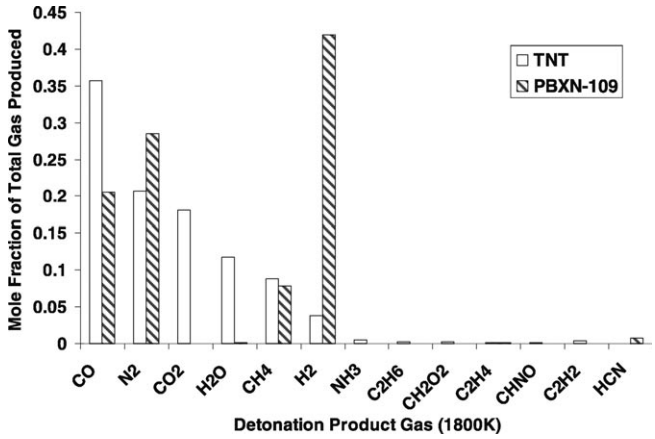

Figure 10. Detonation product gases at 1800 K (freeze out) for TNT and PBXN-109, as predicted by CHEETAH. Note increase in predicted H_2 gas production by PBXN-109, relative to TNT.

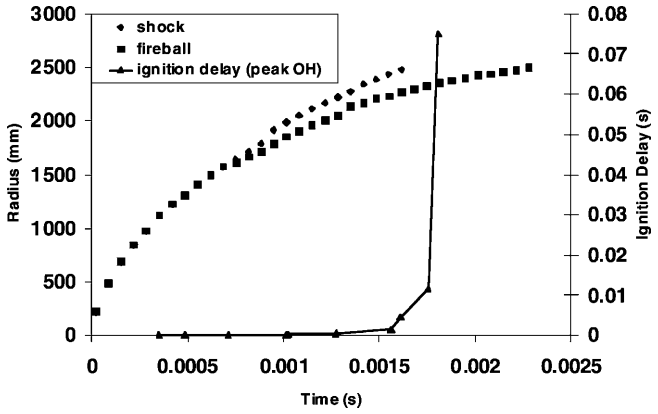

Figure 12. Measured shock and fireball positions for a 2 kg PBXN-109 charge versus distance from charge center, and the ignition delay associated with the gas mixture at that position. Analogous to Figure 8.

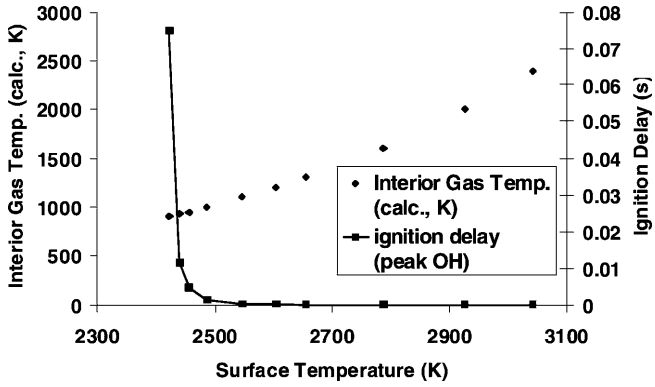

Figure 11. Calculated fireball surface temperature and calculated ignition delay for various interior gas temperatures, for equal volume PBXN-109 detonation product gas/air mixtures. As the preignition temperature increases, the ignition delay decreases and the mixture burns hotter. Analogous to Figure 7.

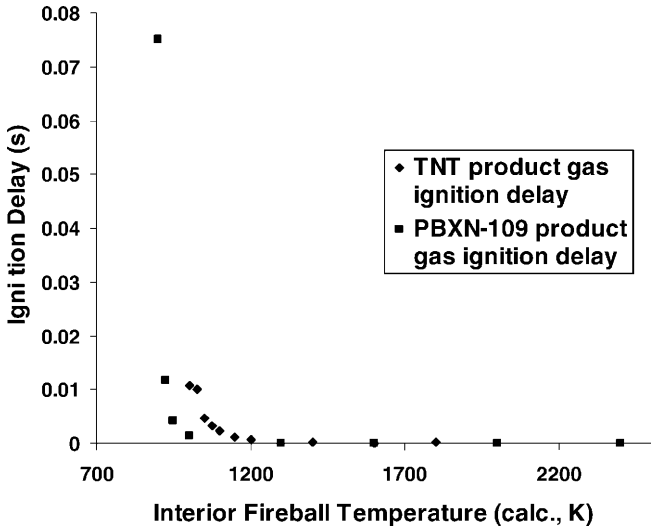

Figure 13. Calculated ignition delay versus interior fireball temperature for equivolume homogeneous TNT detonation product gas/air mixtures and equivolume homogeneous PBXN-109 detonation product gas/air mixtures.

PBXN-109. The implication here is that condensed explosives that exhibit minimal ignition delay in their afterburn have the most potential to maximize middle time shock velocity augmentation, and thus exhibit enhanced blast.

6 Summary and Conclusion

In this paper, we have attempted several things. First, we believe we have proposed a reasonable set of time regimes that describe energy release in unconfined solid explosives. These time regimes are based upon visual records and temperature histories. Most importantly, we think that our proposal to use the time of freeze out as a marker for the beginning of the afterburn and shock-fireball separation as the marker for late time energy release makes sense. Secondly, we propose that enhanced shock velocity in middle time, prior to shock separation, is a metric for enhanced blast. Thirdly, we have shown that the calculations predict different ignition delays for similar volumetric mixtures of air and detonation products from different explosives. In particular, these calculations predict that detonation products enriched in hydrogen have shorter ignition delays than those that do not contain hydrogen, when these products are mixed in similar proportions with air. These results imply that explosive formulations that produce hydrogen-enriched detonation products will ignite in air at lower temperatures than non-hydrogen enriched mixtures. Since the fireball temperatures are a function not only of detonation temperature but also of distance from charge center, explosives that produce hydrogen in their detonation products may be most able to provide shock augmentation at greater distances from the charge center. We suggest that the real meaning of enhanced blast should be some type of middle time shock augmentation as

measured and modeled here. These results suggest a path toward formulation of new enhanced blast explosives. For middle time shock enhancement, the formulation should maximize detonation temperatures while also minimizing ignition delay in detonation product gas/air mixtures. These results suggest maximizing hydrogen content in detonation product gases, but other product gases may also provide increased performance (e.g., CH_4).

Finally, it must be noted that this work has several shortcomings. We believe that chief among these are the lack of incorporation of the chemical kinetic mechanism into a fluid dynamic model (e.g., incorporation into a model similar to that of [6]), and the need to incorporate inhomogeneous kinetics (i.e., burning of carbon particles) into the kinetic model to predict ignition delay of afterburning. The approach used here neglects turbulent mixing and steep pressure and temperature gradients that occur within and between the time regimes proposed here. We are presently attempting to address each of these issues. However, we believe the work here demonstrates the need for the inclusion of chemical kinetics into a fluid dynamic model, and demonstrates that any model that predicts energy release in the time regimes outlined here must not rely solely on equilibrium chemistry.

7 References

[1] K. Kim, Thermobarics: Promises, Challenges and Recommendations, *7th Joint Classified Bombs/Warheads and Ballistics Symposium*, Monterey, CA, August 9 – 12, **2004**.

[2] C. H. Johansson, P. A. Persson (Eds.), *Detonics of High Explosives*, Academic Press Inc., New York **1970**.

[3] P. W. Cooper (Ed.), *Explosives Engineering*, Wiley-VCH, New York **1996**.

[4] R. Cohen, Y. Zeiri, E. Wurzberg, R. Kosloff, Mechanism of Thermal Decomposition of TNT: A DFT Study, *J. Phys. Chem. A* **2007**, *111*, 11074.

[5] A. G. Gaydon, Applications of Spectroscopy to Combustion, *Rep. Prog. Phys.* **1941**, *8*, 50.

[6] A. K. Oppenheim, A. L. Kuhl, Dynamic Features of Closed Combustion Systems, *Prog. Energy Combust. Sci.* **2000**, *26*, 533.

[7] B. E. Gel'fand, M. F. gogulya, S. P. Medvedev, A. N. Polenov, S. V. Khomik, Diagnostics of the Afterburning of the Detonation Products of Condensed Explosives, *Dokl. Phys. Chem.* **2001**, *379*, 186.

[8] R. E. Lottero, B. Krzewinski, K. McNesby, B. Homan, S. Stegall, P. Baker, R. Maulbetsch, *The Physical, Gas-Dynamic, and Instrumentation Design of the ARL Instrumented-Pipe Thermobarics Research Facility*, ARL-TR-3177, U.S. Army Research Laboratory, Aberdeen Proving Ground, MD USA 21005-5066, April, **2004**.

[9] R. E. Lottero, B. Krzewinski, K. McNesby, B. Homan, S. Stegall, E. Summers, E. Wilson, D. Serrano, R. Maulbetsch, W. Slack, R. Thompson, *ARL Research in Thermobaric Phenomenology: The First Phase*, ARL-TR-3218, U.S. Army Research Laboratory, Aberdeen Proving Ground, MD USA 21005-5066, June, **2004**.

[10] K. L. McNesby, B. E. Homan, R. Z. Ehlers, B. A. McAndrew, *Energy Release Mechanisms in Enhanced Blast Explosives: Comparison to TNT*, ARL-TR-4505, U.S. Army Research Laboratory, Aberdeen Proving Ground, MD USA 21005-5066, July, **2008**.

[11] K. L. McNesby, B. E. Homan, T. N. Piehler, R. E. Lottero, *Spectroscopic Measurements of Fireballs Produced by Enhanced Blast Explosives*, ARL Technical Report ARL-TR-3318, U.S. Army Research Laboratory, Aberdeen Proving Ground, MD USA 21005-5066, October, **2004**.

[12] K. L. McNesby, B. E. Homan, T. N. Piehler, R. E. Lottero, *Real-Time Optical Measurements for Improved Understanding of Enhanced Blast Materials*, ARL-TR-3483, U.S. Army Research Laboratory, Aberdeen Proving Ground, MD USA 21005-5066, May, **2005**.

[13] K. L. McNesby, B. E. Homan, R. E. Lottero, *High Brightness Imaging for Real Time Measurement of Shock, Particle, and Combustion Fronts Produced by Enhanced Blast Explosives*, ARL-TR-3411, U.S. Army Research Laboratory, Aberdeen Proving Ground, MD USA 21005-5066, January, **2005**.

[14] K. L. McNesby, A. W. Miziolek, T. Nguyen, F. C. Delucia, R. R. Skaggs, T. A. Litzinger, Experimental and Computational Studies of Oxidizer and Fuel Side Addition of Ethanol to Opposed Flow Air/Ethylene Flames, *Combust. Flame* **2005**, *142*, 413.

[15] K. N. Bray, N. Peters, Laminar Flamelets in Turbulent Flames, in: P. A. Libby, F. A. Williams (Eds.), *Turbulent Reacting Flows*, Academic Press, New York, **1994**.

Acknowledgements

This work was partly supported by the Defense Threat Reduction Agency (DTRA). Richard Lottero contributed to this work.

